

FORMATION OF GLOBULAR STRUCTURES IN ALUMINUM A356 ALLOY BY NARROW MELT STREAM (NMS) TECHNIQUE

A. H. Shafie Farhood and F. Akhlaghi

fakhlagh@ut.ac.ir

Received: August 2009

Accepted: January 2010

School of Metallurgy and Materials Engineering, Faculty of Engineering, University of Tehran, P.O. Box: 11365-4563, Tehran, Iran

Abstract: Narrow Melt Stream (NMS) is a relatively new semisolid metal processing technique for producing globular structures in alloys. This method is based on pouring the melt through a small sized nozzle into a mould located at a certain height under the crucible. This simple method generates globular structures without using equipments such as impellers, electromagnetic stirrers, ultrasonic probes and cooling slopes. Therefore it is cost effective. In the present study, the effect of casting size and mould casting modulus on the globular structure evolution in A356 aluminium alloy specimens prepared by NMS process was investigated. The results showed that regardless of the different casting modulus and their sizes, all the specimens exhibited globular structures. However, the size and shape factor of the globules decreased with increased casting modulus and casting size indicating the influential effect of the surface area of the mould in generating globular structures in this process.

Keywords: Narrow Melt Stream (NMS), Casting Modulus, Casting Size, Globule Size, Globule Shape.

1. INTRODUCTION

The cooling rate during solidification, which is mainly controlled by the mould geometry, is one of the most influential factors affecting the final microstructure of the cast alloys [1]. Generally speaking, in addition to the alloy system, solute gradient and its diffusivity ahead of the solidification front, the microstructure of solidified alloys are largely dependent on the rate of heat extraction from the mould or solidification rate [2, 3]. It has been shown that the solidification rate is proportional to the n^{th} power of the ratio (V/A) as the casting modulus M , where V is the casting volume and A is the effective cooling surface area. Based on Chvorinov's equation, the solidification time of a casting, t_f , is related to its modulus, $t_f = k_0 M^2$, where k_0 is a constant depending on the cast metal and mould material properties [4, 5]. Although the Chvorinov's equation was introduced to the open literature during the 1940s, but nowadays, after nearly seven decades, it is still being used in modeling and designing of risering and gating systems. The microstructure and mechanical properties of the castings are highly influenced by the casting modulus. Yokota and co-workers [5] investigated the effect of the casting modulus on the scale of microstructure of Al-8.45Si-2.35Cu alloy by

measuring the dendrite arm spacing (DAS) and showed an effective relationship between the casting modulus, cooling rate, microstructure and strength of the castings.

Semi-solid processing (SSP) is believed as a promising near-net shape forming technology for its unique features compared with conventional metal forming methods. In SSP a suitable volume fraction of fine and spherical particles (globules) are dispersed uniformly in a liquid matrix. It is reported that SSP takes many advantages over the conventional forming process, such as longer die life, better surface finish, improved mechanical properties, better dimensional tolerance, faster production cycle, net shape casting, less porosity, reduced macrosegregation, lower forming temperature and lower energy consumption [6, 7]. There are two primary semi-solid processing routes, (a) rheocasting and (b) thixocasting. In the rheocasting route, one starts from the liquid state, and in order to produce a non-dendritic microstructure, a high shear rate is applied to the solidifying alloy. Therefore, the thixotropic slurry is formed directly from the melt and the slurry is subsequently fed into the die cavity. Several methods have been reported to successfully produce the thixotropic structure in aluminium alloys using this processing route. These include mechanical stirring [8], electromagnetic stirring

[9] and twin screw process [9]. In the thixocasting route, one starts from a solid precursor material that is specially prepared by a primary manufacturer. Upon reheating this material into the mushy (two-phase) zone, a thixotropic slurry is formed, which becomes the feed for the forming operation. A number of methods have been reported that rely on this route; such as slope casting [11, 12], strain induced melt activation (SIMA) [13] and Narrow Melt Stream (NMS) process [14].

The NMS technique is a new semi-solid processing route which was developed in the school of Metallurgy and Materials Engineering, University of Tehran [14]. This method is based on pouring the melt through a small sized nozzle into a mould located at a certain height under the crucible. The controlled nucleation events promoted by the interaction of the melt stream upon entering the mould cavity, together with generation of nuclei upon contact of the melt with the mould bottom and walls, provide a suitable non-dendritic microstructure which can be converted to a globular structure after reheating. In the previous investigations, the effects of some processing parameters of the NMS process such as the degree of the melt superheat, melt delivery nozzle diameter and melt stream height on the globular structure of aluminium 356 alloy was reported. However, in those experiments a specified mould of certain dimensions was used and the applicability of the NMS method in producing globular structures by using various mould dimensions was not explored.

The aim of the present study is a systematic investigation on the effects of mould size and modulus of casting on the size and morphology of the globular structures formed by NMS processing of Al 356 alloy. For this purpose, six different series of moulds with identical casting modulus but different volumes were employed.

2. EXPERIMENTAL PROCEDURE

a: Mould Design

In this study, cylindrical moulds having diameter of (d) and height of (h) were used.

Since the heat is extracted from the solidifying melt mainly through the base and wall of the mould, its effective cooling surface area is (A) and its casting modulus is calculated by using the following equation:

$$M=V/A=(\pi d^2h/4)/(\pi d^2/4+\pi dh) \quad (1)$$

Or

$$M=dh/(d+4h) \quad (2)$$

Or

$$d=4hM/(h-M) \quad (3)$$

By substituting (d) from Eqn. 3 in the relevant equation for calculating the volume of a cylinder, the following Eqn. is obtained:

Table 1. The characteristics of cylindrical moulds used in this study

Sample code	d(Cm)	h(Cm)	V(Cm ³)	M(Cm)	$\Delta V_{(max)}$ (%)
M ₁₋₁	6.0	3.0	85	1.0	58.5
M ₁₋₂	4.6	8.0	130	1.0	
M ₁₋₃	4.4	14.0	205	1.0	
M _{1.2-1}	7.2	3.6	150	1.2	53.1
M _{1.2-2}	5.6	8.0	200	1.2	
M _{1.2-3}	5.2	15.0	320	1.2	
M _{1.4-1}	8.4	4.2	235	1.4	42
M _{1.4-2}	6.3	12.0	380	1.4	
M _{1.4-3}	6.3	13.0	405	1.4	
M _{1.6-1}	9.8	5.0	350	1.6	42.1
M _{1.6-2}	7.8	9.0	430	1.6	
M _{1.6-3}	7.2	15.0	605	1.6	
M _{1.8-1}	10.8	4.4	495	1.8	38.0
M _{1.8-2}	8.7	10.0	605	1.8	
M _{1.8-3}	8.2	15.0	800	1.8	
M ₂₋₁	12.0	5.9	680	2.0	32.0
M ₂₋₂	10.0	10.0	785	2.0	
M ₂₋₃	9.5	14.0	1000	2.0	



Fig. 1. The variation of the volume of the cylindrical moulds versus their height for different series of moulds having various casting modulus ranging from 1 to 2.

$$V = 0.25 \pi h (4hM / (h-M))^2 \quad (4)$$

By using the above Eqn. the variation of (V) versus (h) can be plotted for different values of (M) as shown in Fig. 1.

The dimensions of 18 moulds were selected according to Fig. 1, which could be classified in 6 series as shown in Table 1. Each series included 3 moulds having constant modulus but different volumes. The moulds are designated by M_x-y in which x is the casting modulus and y is the mould number in each series which increases with the volume of the mould. The cast iron moulds were prepared by using wooden patterns, sand casting and machining. The base and wall thickness of all the machined moulds were about 5 mm and all of them had a slope of 1.5° to facilitate the removal of the casting from the mould. In order to prevent welding of the casting to the mould, the mould cavity was coated with a Zirconia based coating material (Holcote 110) prior to each melt pouring.

b: Processing and Microstructural Characterisation

In the present investigation, aluminium 356 alloy produced by “Arak Amijeh Saz co., Iran”,

having the nominal chemical composition as shown in Table 2 was used. The liquidus and solidus temperatures of this alloy as quantified by thermal analysis technique were 611°C and 573°C respectively.

The required amount of the alloy ingot was charged in a graphite crucible and heated at 650°C using a resistance furnace. The melt was then transferred to a bottom pouring crucible having a 10 mm nozzle at the centre of its base. This crucible was preheated at 650°C using the same furnace. The melt was ejected through the nozzle simply by its own weight (gravity pouring) and poured into a mould located at 1500mm below the melt delivery nozzle. Samples were cut from the geometrical centre of the solidified ingots as shown in Fig. 2. The dark region as shown in the Fig. 2-c was subjected to heat treatment at 580°C for 8 min followed by water quenching [15]. The re-heated samples were subjected to standard metallographic procedures and etched by using 0.5%HF solution. The microstructure of samples was studied using a “Ziess” light microscope. For image processing of the resulted microstructures, for each sample, a total number of 100 randomly selected globules were analyzed using “Image Tools” software with the total measured area of 300 mm^2 per specimen.

The size and shape factor of globules were quantified by measuring the perimeter (P_g) and surface area (A_g) of primary $\alpha\text{-Al}$ particles. Then the effective diameter (D_e) and shape factor (S_F) of the globules were calculated according to the following equations:

Table 2. Chemical composition (in wt.%) of aluminium 356 alloy

Si	Fe	Mg	Zn	Cu	Mn	Ti	Al
6.93	0.44	0.38	0.26	0.2	0.13	0.09	rem

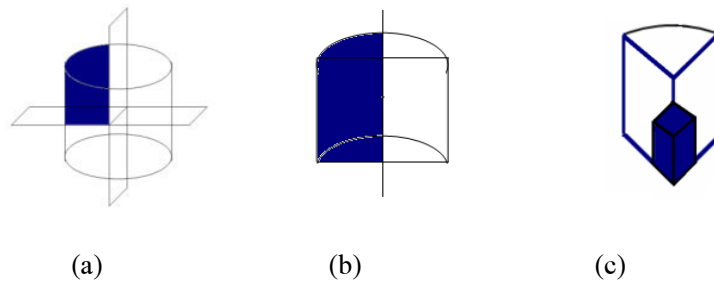


Fig. 2. (a – c) showing the sequence of sectioning the cylindrical samples for preparation of metallographic specimens

$$D_e = 4A_g / P_g \quad (5)$$

$$SF = 4A_g \pi / P_g^2 \quad (6)$$

The standard deviation values obtained for each measurement was used for estimating the experimental errors.

3. RESULTS AND DISCUSSIONS

The microstructures of the different re-heated samples obtained from various moulds are shown in the Fig. 3. It can be seen that regardless of a relatively wide range of both casting volumes (85-1000 Cm^3) and modulus (1-2 Cm) all the samples exhibited globular structures confirming the applicability of the NMS process in producing globular structures for a range of solidification rates.

The average size and shape factor of globules in different samples are listed in Table 3. It can be observed that for each mould series having identical casting modulus but different volumes, the effective diameter of the globules (D_e) has not changed considerably and their scatter is within the experimental errors. A comparison between the microstructure of different samples in each series of Fig. 3 also reveals the relatively constant size of the globules obtained in the samples with identical casting modulus. According to Table 3, the maximum divergence in the volumes of samples in each mould series (ΔV_{max}) is less than 60%. In order to see the net effect of the casting modulus on the size of globules, one can compare samples $M_{1.6-1}$ and $M_{1.8-3}$ having the volumes of 350 Cm^3 and 800 Cm^3 respectively. The divergence in the volumes of these samples is only about 56% but the globule size of the

Table 3. The average size and shape factor of globules generated in different mould series

Sample code	Average D_e globule size (μm)	SF shape factor
M_{1-1}	53 ± 2	0.85 ± 0.02
M_{1-2}	57 ± 2	0.81 ± 0.02
M_{1-3}	55 ± 2	0.79 ± 0.02
$M_{1.2-1}$	54 ± 2	0.83 ± 0.02
$M_{1.2-2}$	53 ± 2	0.80 ± 0.02
$M_{1.2-3}$	59 ± 3	0.79 ± 0.02
$M_{1.4-1}$	56 ± 2	0.85 ± 0.02
$M_{1.4-2}$	57 ± 2	0.82 ± 0.02
$M_{1.4-3}$	61 ± 2	0.72 ± 0.02
$M_{1.6-1}$	57 ± 2	0.76 ± 0.02
$M_{1.6-2}$	56 ± 2	0.85 ± 0.02
$M_{1.6-3}$	60 ± 2	0.77 ± 0.02
$M_{1.8-1}$	61 ± 2	0.71 ± 0.02
$M_{1.8-2}$	63 ± 3	0.73 ± 0.02
$M_{1.8-3}$	62 ± 2	0.72 ± 0.02
M_{2-1}	67 ± 3	0.68 ± 0.03
M_{2-2}	63 ± 3	0.70 ± 0.03
M_{2-3}	69 ± 3	0.70 ± 0.03



Fig. 3. Showing the microstructure of the different re-heated samples obtained from various moulds according to Table 3

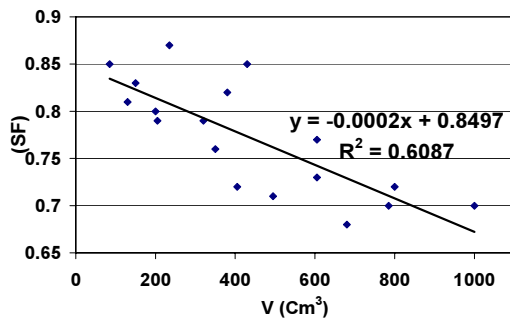
larger sample ($62 \pm 3 \mu\text{m}$) is significantly larger than that of the smaller one ($57 \pm 2 \mu\text{m}$) as shown in the corresponding micrographs (Fig. 3).

The same trend is observed in the samples

$M_{1,8-1}$ and M_{2-3} having the volumes of 495 Cm^3 and 1000 Cm^3 respectively resulting in a volume divergence of 50.5%. According to the Table 3, the D_c values of these samples are $61 \pm 2 \mu\text{m}$ and



(a)



(b)

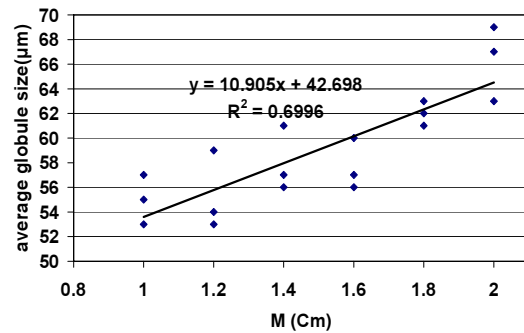
Fig. 4. The variation of (a) size and (b) shape factor of globules with the volume of the moulds.

$69 \pm 2 \mu\text{m}$ and a comparison between the corresponding micrographs of Fig. 3, clearly reveals the larger size of the sample with a larger casting modulus. In this respect, it is interesting to compare samples M_1-1 and M_1-3 . In spite of a relatively large volume divergence ($\Delta V = 58.5\%$) these samples exhibited nearly equal D_e values ($53 \pm 2 \mu\text{m}$ vs. $55 \pm 2 \mu\text{m}$) attributable to their identical casting modulus. Therefore, it can be concluded that the size of globules in each mould series with the mentioned volume deviations was not affected by the size of the casting. However, samples with different casting modulus exhibited different globule sizes despite a relatively low volume divergence.

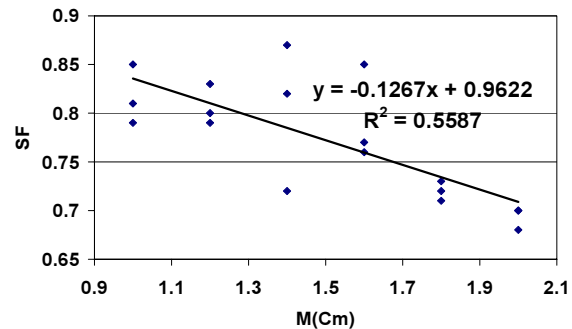
As shown in Table 3, in each mould series with a casting modulus less than 1.6 Cm, the shape factor of globules decreased with increased sample volume. However, for the mould series with larger modulus, the shape factor remained constant in each series. These observations can be attributed to the generation of different as-cast microstructures

in the various samples. In other words, in each mould series, the increased mould volume resulted in a more pronounced preferred orientation of primary α -Al particles due to the extended solidification time. This effect manifested itself in forming less spherically shaped globules after re-heating. However, when the casting modulus was relatively large, (i.e. $M \geq 1.6 \text{ Cm}$), the effect of the casting volume on the shape factor of the globules was negligible and all of the samples exhibited relatively low SF values.

In order to investigate the effectiveness of the casting size in the NMS process in generating high quality globular structures, the variation of the size and shape factor of globules are plotted against the volume of moulds regardless of their casting modulus as shown in the Fig. 4(a and b). Similarly, the variation of G_e and SF vs. casting modulus, regardless of their volumes are shown in the Fig. 5(a and b).



(a)



(b)

Fig. 5. The variation of (a) size and (b) shape factor of globules with the casting modulus of the moulds.

As was expected, the size of globules increases and their shape factor decreases with increased volume and/or modulus of the moulds. However, the higher co-relation factors obtained for Fig. 4 as compared with those of Fig. 5 indicate the more influential effect of the casting size, (as compared with the casting modulus) on the size and shape of globular structures generated within the present set of experimental data and conditions.

According to Chvorinov's equation, the solidification time of a casting is proportional to its squared casting modulus. As was mentioned before, the extended solidification time results in a coarser and more oriented microstructure in the as-cast condition. Therefore, larger globules with decreased shape factors can be anticipated for longer solidification times. The plots of G_c and SF against M^2 (which is proportional to the solidification time), are shown in the Fig.6 (a and b) and confirm the strong relationship between

the solidification time and the size and morphology of the resultant globular structures. The higher co-relation factors obtained for Fig.6 as compared with those of Fig. 5, reveals that the effect of casting modulus on the size and morphology of castings is imposed via its effect on the solidification time.

The variation of the average size and shape factor of globules with the casting modulus of each mould series is shown in Fig. 7(a and b). It can be seen that, by considering the error bars, the increased casting modulus up to 1.6 Cm, did not have any considerable effect on the size and/or shape factor of the globules. However, further increase in the casting modulus, imposed a sharp increase in the D_c and a significant decrease in the SF values. The same trend is observed in Fig. 8(a and b), indicating relatively constant values for the average size and average shape factor of globules in each mould series

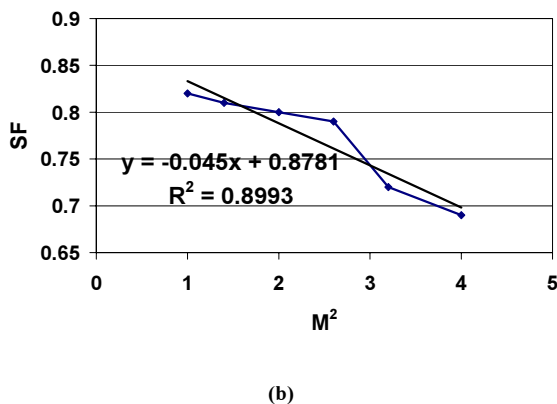
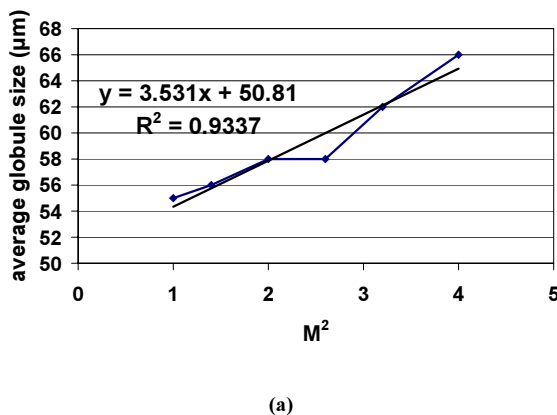


Fig. 6. The variation of (a) size and (b) shape factor of globules with M^2 .

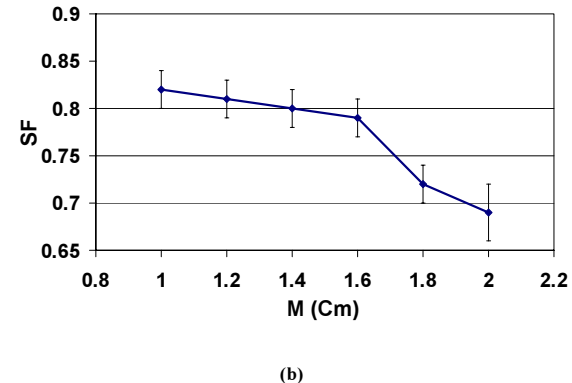
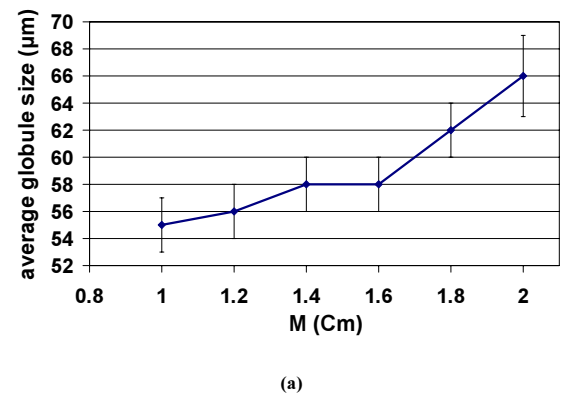


Fig. 7. The variation of (a) size and (b) shape factor of globules with the casting modulus of each mould series.



Fig. 8. The variation of (a) size and (b) shape factor of globules with the average volume of the moulds.

when they were plotted against the average volume of the moulds. In this case, the critical mould volume is about 500 Cm^3 beyond which a steep increase in the size and a sharp decrease in the shape factor of the globules have occurred.

4. CONCLUSIONS

In this study the NMS process was applied to aluminium 356 alloy poured in 18 moulds (with different dimensions classified in 6 series with identical casting modulus) and the applicability of this technique in generating globular structures for the whole range of mould dimensions was demonstrated. The following conclusions have been drawn from this work:

1. The size of the globules generated in each series of moulds with an identical casting modulus and a maximum mould volume deviation of about 60% remained relatively constant. However, for the mould series having a casting modulus smaller than 1.6 Cm , the increased size of the moulds resulted in decreased shape factor of globules.
2. The increased casting modulus of the moulds resulted in increased size and decreased shape factor of globules even though the increased mould volume was not significant.
3. The increased volume and/or modulus of the moulds resulted in increased size and decreased shape factor of the globules. However, within the present set of experimental data and conditions, the influence of the mould volume on the size and shape factor of the globules was stronger as compared with the casting modulus.
4. The strong relationship between the solidification time (which is proportional to the squared casting modulus) and the size and morphology of the resultant globular structures was confirmed.
5. There exists a critical mould volume ($\sim 500 \text{ Cm}^3$) and a critical casting modulus (1.6 Cm), beyond which the average values of the globule sizes and globule shape factors in each mould series (with identical casting modulus), change considerably. However, below these critical values, the globules exhibit nearly constant size and shape factors.

ACKNOWLEDGMENT

The authors would like to acknowledge the financial support of the Centre of Excellence for High Performance Materials, University of Tehran.

REFERENCES

1. Hedjazi, J., Solidification and Metallurgical Principles of Founding, 5th ed., IUST, Tehran,

- Iran, 2000, pp. 209-221.
2. Flemings, M.C., *Behaviour of Metal Alloys in the semi-solid state. Metall. Trans. A*, 1991, **22A**, 957.
3. Hellawell, A., *Mechanical deformation of dendrites by fluid flow. Metall. Trans. A*, 1996, **27A**, No.1, 229.
4. Chvorinov, N., Theory of solidification of casting. Giesserei, 1940, **27**, 177.
5. Yokota, S., and Mizuno, K., *Effect of casting modulus on structure and mechanical strength of AC4B Aluminium alloy square column castings. J. Japan Inst. Light Metal.*, 2000, **50**, No.5, 198.
6. Fan, Z., Semisolid Metal Processing. *Internat. Mater. Rev.*, 2002, **47**, No. 2, 1.
7. Atkinson, H.V., *Modelling the semisolid processing of alloy. Prog. Mater. Sci.*, 2005, **50**, 341.
8. Sukumaran, K., Pai, B. C. and Chakraborty, M., *The Effect of Isothermal Mechanical stirring on an Al-Si Alloy in the Semisolid Condition. Mater. Sci. Eng.A.*, 2004, **369**, 275.
9. Seo, P.K., Kim, B.M. and Kang, C. G., "The Comparison of Reheating Process in A356 Alloy Manufactured by Electromagnetic Stirring and Extrusion for Semisolid Forming" *Proceedings of the 8th International Conference on Semisolid Processing, University of Cyprus, Cyprus, Limassol*, 2004.
10. Ji, S., Fan, Z., and Bevis, M.J., *Semisolid processing of engineering alloys by twin screw rheomoulding process. Mater. Sci. Eng. A.*, 2001, **2999**. Issue 1-2, 210.
11. Salarfar, S., Akhlaghi, F. and Nili-Ahmadabadi, M., "Influence of Pouring Conditions in the Inclined Plate Process and Reheating on the Microstructure of the Semisolid A356 Aluminium Alloy" *Proceedings of the 8th International Conference on Semisolid Processing, University of Cyprus, Cyprus, Limassol*, 2004.
12. Haga, T. and Suzuki, S., *Casting of Aluminium Alloy Ingots for Thixoforming Using a Cooling Slope, J. Mater. Proc. Technol.*, 2001, **118**, 169.
13. Turkeli, A. and Akbas, N., "Formation of non-dendritic structure in 7075 wrought aluminium alloy by SIMA process and effect of heat treatment" *Proceedings of the 4th Internat. Conf. on Semisolid Processing of Alloys and Composites, Sheffield*, 1996, 71-74.
14. Shahriary, B., "The Semisolid Processing of Aluminum Alloys by using Narrow Melt Stream Method", M.Sc. Thesis, University of Tehran, Iran, 2007.
15. Shahriari, B. and Akhlaghi, F. " Optimization of heat treatment for obtaining globular structures in Al A356 alloy" *Proceedings of the 7th National Conference on Surface Engineering and Heat Treatment, School of Materials Engineering, Isfahan University of Technology, Isfahan, Iran*, 3-4 May 2006.